Journal of the Korean Crystal Growth and Crystal Technology
Vol. 26, No. 2 (2016) 67-73
http://dx.doi.org/10.6111/JKCGCT.2016.26.2.067

p-ISSN 1225-1429
e-ISSN 2234-5078

Thermal shock behaviors of TiN coatings on Inconel 617 and Silicon wafer substrates with finite element analysis method

Ki-Seuk Lee[*,**], Seol Jeon[***], Hyun Cho[****] and Heesoo Lee[***,†]

*School of Convergence Science, Pusan National University, Busan 46241, Korea
**Certification Evaluation Center, Korea Testing Laboratory, Jinju 52852, Korea
***School of Materials Science and Engineering, Pusan National University, Busan 46241, Korea
****Department of Nanomechatronics Engineering, Pusan National University, Gyeongnam 50463, Korea

(Received March 21, 2016)
(Revised March 31, 2016)
(Accepted April 8, 2016)

Abstract The degradation behaviors of TiN coating layers under thermo-mechanical stress were investigated in terms of comparison of finite element analysis (FEA) and experimental data. The coating specimen was designed to quarter cylinder model, and the pulsed laser ablation was assumed as heat flux condition. The FEA results showed that heat accumulation at the center of the laser-ablated spot occurred and principle stress was concentrated at the lower region of the coating layer. The microstructural observation revealed that surface melting and decrease of the coating thickness occurred in the TiN/Inconel 617 and the interfacial cracks formed in the TiN/Si. The delamination was caused by the mechanical stress from the center to the outside of the ablated spot as the FEA results expected. It was considered that the improvement of the thermal shock resistance was attributed to higher thermal conductivity of Si wafer than that of Inconel 617.

Key words TiN coating, Thermal shock behavior, Finite element analysis, Thermal conductivity

1. Introduction

Ti-based hard coatings are widely used for various industries due to its excellent properties such as hardness, thermal and corrosion stability, and wear resistance [1-3]. Titanium nitride (TiN) is a representative protective layer for cutting tools, die, and molds so the degradation behaviors of the coating have been investigated under repeated thermal and/or mechanical stresses [4-6]. Other studies have used various techniques to characterize TiN coatings on different substrate materials by applying mechanical or thermal stresses, and the physical properties of the substrate materials influenced to the degradation behaviors of the coating/substrate system [7-10].

Under the practical conditions of the coating, the repeated thermo-mechanical loads can lead to coating failures such as cracking, spalling and delamination. Therefore, it is important to understanding the degradation behavior of the coating under stresses that are close to the practical conditions to assess durability and reliability of the coating materials prior to its application. Pulsed laser ablation method can induce repeated thermo-mechanical stress on the local region of coating surface in a short period of time so that it efficiently simulates the practical conditions of the coating layer [11-13]. Finite element analysis (FEA) method has been considered as a useful tool for expecting the change of temperature and stress by thermal and/or mechanical loads since the accurate measurement of the temperature and load in the cutting zone is difficult [14-16]. FEA can also be used to determine the stress and temperature distributions in laser-ablated spots [17-19].

The purpose of this study is to investigate the effects of substrate materials on the degradation behavior of TiN coatings under repeated thermo-mechanical stress. Inconel 617 was chosen as a metallic substrate material with a high thermal fatigue resistance. Silicon wafer, which has been used as a representative substrate for many studies about coating materials, was also used for comparable study. FEA modeling was conducted by using ABAQUS/CAE™ with consideration of various properties of each material. Surfaces and cross-sections of ablated spots of the TiN coatings on each substrate were observed by scanning electron microscopy (SEM) and focused ion beam (FIB) milling technique to compare the results of the FEA modeling and the experimental data.

†Corresponding author
E-mail: heesoo@pusan.ac.kr

2. Experimental Procedures

TiN coatings with ~2 μm in thickness were deposited onto Inconel 617 (austenitic nickel-chromium based superalloy) and a polished single crystalline silicon (a tetravalent metalloid) wafer at substrate temperature of 450°C by arc discharge technique. The overall substrate dimensions were 20 × 30 × 1 mm, and arc current of 50 A and sputter current of 1.0 A were applied for the deposition process. To enhance adhesion between the coating layer and the substrate, the substrate surfaces were sputter-cleaned by exposure to argon ions at 800 V for 10 min to remove any contaminants.

An Nd-YAG laser ablation system (LSX-213, CETAC Technologies) with a flat-top profile was used to apply the repeated thermo-mechanical shock to the prepared coating specimens, which can control energy output, beam spot size, and the number of pulses based on a computer-based operating program. The ablation diameter was 200 μm, and the number of pulses was increased from 1 to 20 times with an energy output of about 13 J/cm^2 at a 100 % output level with a wavelength of 213 nm. Laser irradiance was ~2 GW/cm^2 with a pulse width of ~5 ns, and the number of laser ablation pulses was increased with a frequency of 1 Hz [12, 13, 19]. As a result of our previous finite element method, maximum temperature on the TiN coating surface was about 14,000 K with Gaussian distribution. It was calculated by laser irradiance (~2.6 GW/cm^2) which is obtained from laser fluency (J/cm^2) by dividing by the pulse width (5 ns) with major physical properties of TiN [20].

FEA using ABAQUS/CAE™ simulated the pulsed laser ablation process as a uniform heat flux to the coating surface based on laser energy flux (W/cm^2). The specimens were modeled to quarter cylinders and matched the size of the experimental specimens [21, 22] and the maximum temperature and principal stress were calculated during the short ablation times (5 ns). Table 1 shows the major physical properties of the coating and the substrates in the FEA model [19, 23]. The 1st order 8-noded thermally coupled brick element (tri-linear displacement and temperature system, C3D8T) was used in the modeling, and total nodes were 26,578 (total elements: 23,564, thermal gap conductance: 50,000 W/μm · °C for 0.1 mm). Contact property of the coating and the substrate was chosen by cohesive behavior, and geometric boundaries were riveted as the X and Y axes with zero in displacement for each other. Each part and the assembled model of the coating/substrate specimen were shown in Fig. 2.

Table 1
Material properties used in the FEA simulation of coating specimen

Material	Titanium nitride	Inconel 617
Density (g/cm^3)	5.22	8.36
Elastic modulus (GPa)	251	211
Specific heat (J/Kg · °C)	602	419
Linear thermal expansion coefficient (1/°C)	9.35 × 10^{-6}	11.6 × 10^{-6}
Thermal conductivity (W/m · °C)	19.2	13.4
Poisson's ratio	0.25	0.30

The degradation behaviors of the coating/substrate systems according to laser pulses were observed using scanning electron microscopy (S-4800, Hitachi) and focused ion beam (Nova 200 NanoLab, FEI) milling technique. The width length and the depth of the FIB milling were ~10 and 5 μm, respectively, and Fig. 3 shows an example of the milling procedure at the laser-ablated spots for observing the interfacial regions of the coating specimens.

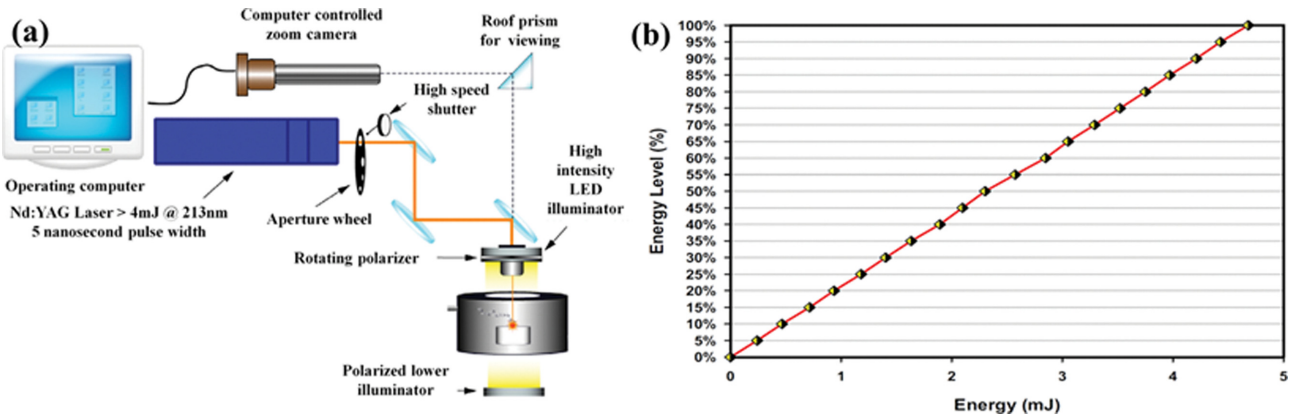

Fig. 1. LSX-213 pulsed laser ablation system: (a) schematic of operation and (b) linear output of laser energy.

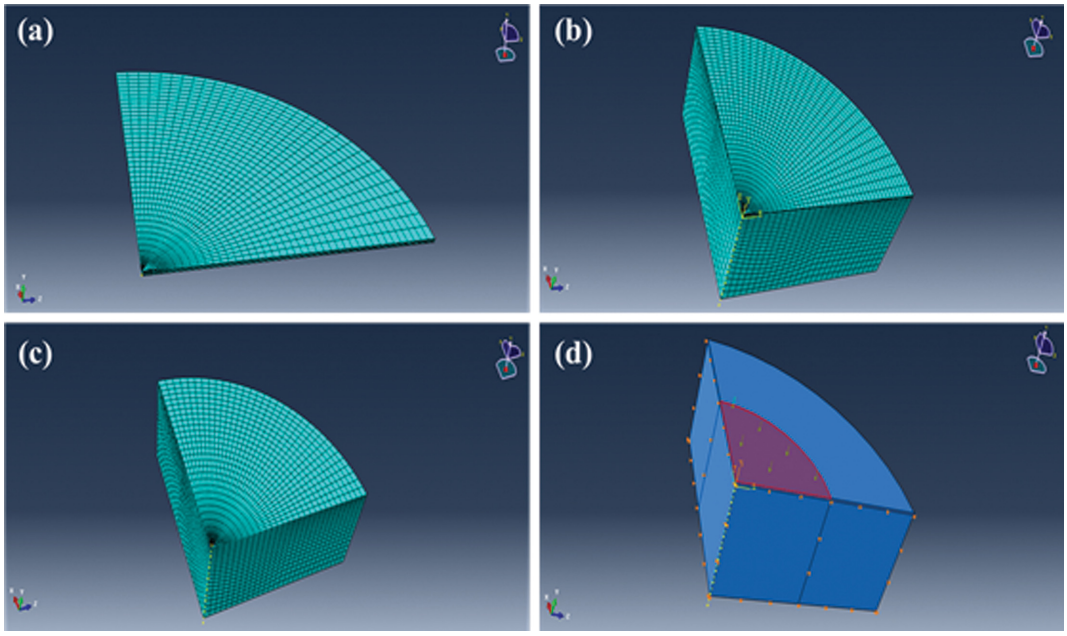

Fig. 2. FEA modeling of the coating specimen with laser ablation: (a) coating part, (b) substrate part, (c) assembled specimen, and (d) stress induce as heat flux.

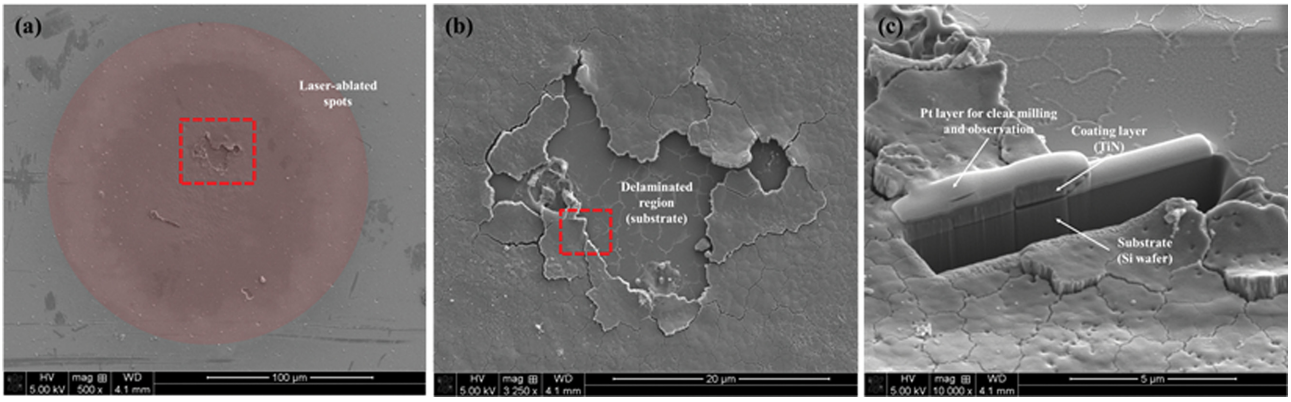

Fig. 3. Example of FIB milling to the ablated spot in TiN coating on Si wafer after 20 pulses: (a) laser-ablated spot, (b) delaminated region in the spot, and (c) a tilted image of the specimen.

3. Results and Discussion

Fig. 4 shows the results of the FEA simulation - the distribution of temperature and principle stress after the laser ablation of one pulse as a uniform heat flux to the coating surface. The heat accumulation was identified at the center of the laser-ablated spot (seen in Fig. 4(a)), and the principle stress was propagated to a direction of depth and concentrated at the lower regions of the coating layer as shown in Fig. 4(b). This FEA results indicated that the repeated thermo-mechanical shock can occur a melting of the coating surface from the center of the ablated spot and a delamination of the coating layer from the coating/substrate interfacial region.

To identify the accordance between the FEA results and the experimental data, the degradation behavior of each coating specimen was investigated by observing the changes in morphology. Fig. 5 shows the degraded surface of the coating specimens after the repeated pulsed laser ablation. In the TiN/Inconel 617 specimen, the surface cracks was formed by the laser thermal shock and the size of the surface crack was increased as the laser pulses increase (in Fig. 5(a) and (b)), while the delamination with melting of the coating surface occurred as seen in Fig. 5(c) after 15 pulses. In the case of the TiN/Si wafer specimen, less surface cracks was observed after same laser pulses as shown in Fig. 5(d) and (e), and the delamination of the coating layer without the surface melting occurred at further laser pulses (in Fig. 5(f)).

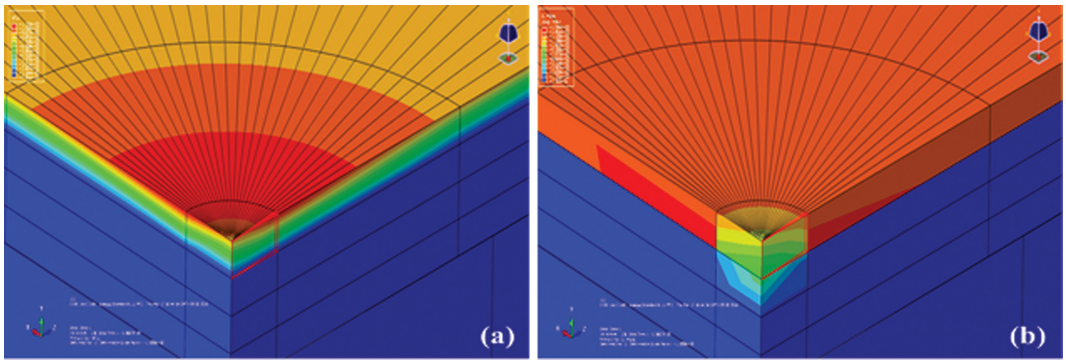

Fig. 4. Visualization of the laser-ablated coating specimen: (a) Temperature and (b) principle stress distribution after laser pulse.

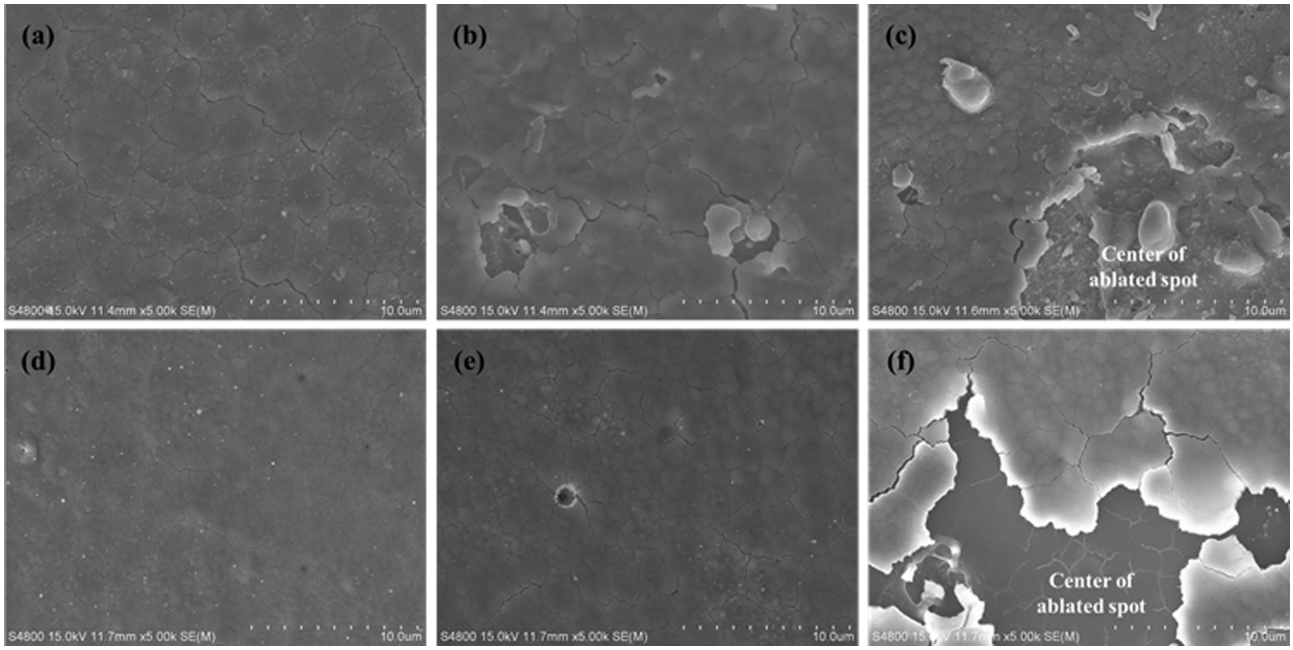

Fig. 5. Surfaces of laser-ablated spots on the coating specimens: after (a) 5, (b) 9, (c) 15 pulses to TiN on Inconel 617, (d) 9, (e) 15, (f) 20 pulses to TiN on Si wafer.

Fig. 6 shows the surface and the cross-sectional images of the degraded spot after 15 pulses of the laser ablation according to distance from the center of the spot. As seen in Fig. 6(b), the coating layer was completely removed after 15 laser pulses. The intercolumnar cracks from the coating surface were observed in the outside of the laser-ablated spot as the white arrows indicated (in Fig. 6(c)). The delamination of the coating layer occurred with the cracks which penetrated the whole coating layer as shown in Fig. 6(d), and it indicates that the mechanical stress was generated by the laser ablation from the center to the outside of the spot [11, 24]. In accordance with the FEA simulation (Fig. 4), the melting of the coating surface at the center of the ablated spot and the delamination of the coating layer occurred after the repeated laser ablation.

Cross-sections of the ablated spots were observed in order to compare the degradation of the coating/substrate system according to the thermal properties of the substrates. The thickness of coating layer was decreased and the roughness of coating surface was increased as the laser pulses increased in the TiN/Inconel 617 specimen as seen in Fig. 7(a) and (b). The removal of the coating layer can be explained as follows; after the laser ablation, a thermal penetration layer with high temperature and superheated liquid is formed at the surface and thermal diffusion of the layer in a direction to the substrate from the surface occurred [25]. The melting of coating surface only in the TiN/Inconel 617 specimen can be explained by the difference of thermal conductivity (Inconel 617: 13.4, Si wafer: 148 W/m · ^{o}C) which allowed more heat accumulate on the coating surface.

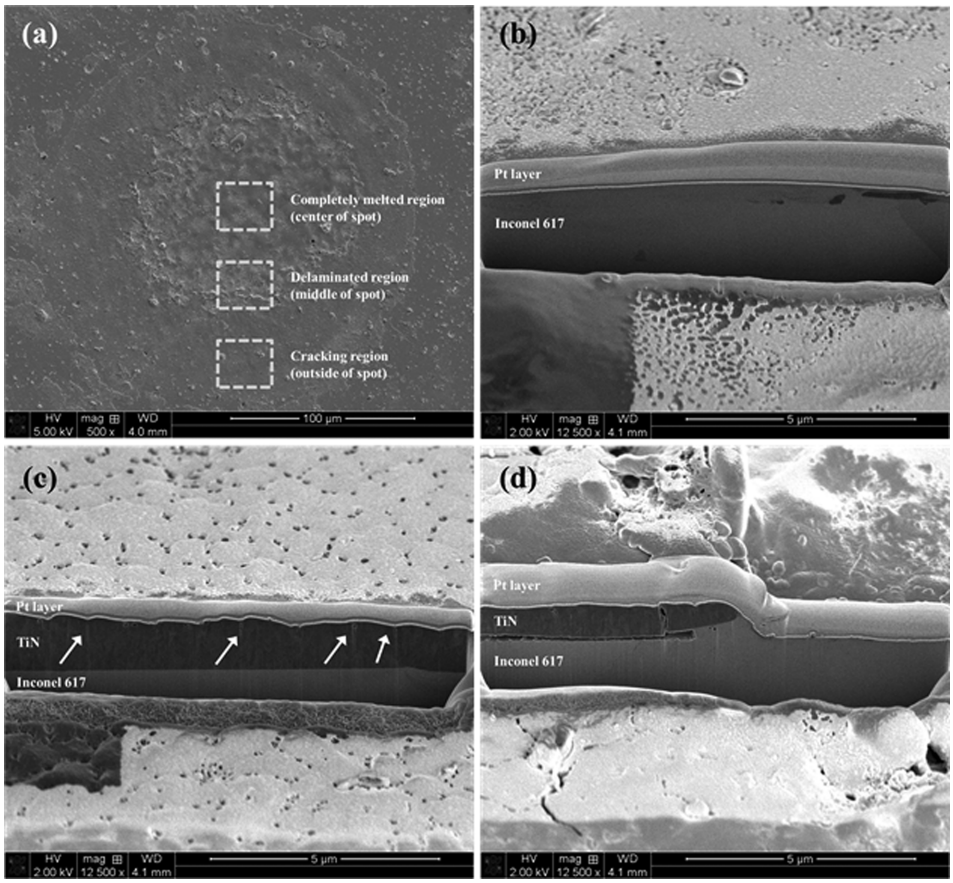

Fig. 6. The ablated spot of TiN coating on Inconel 617 after 15 pulses: (a) surface of the ablated spot, (b) cross-section of center, (c) outside, and (d) middle in the spot.

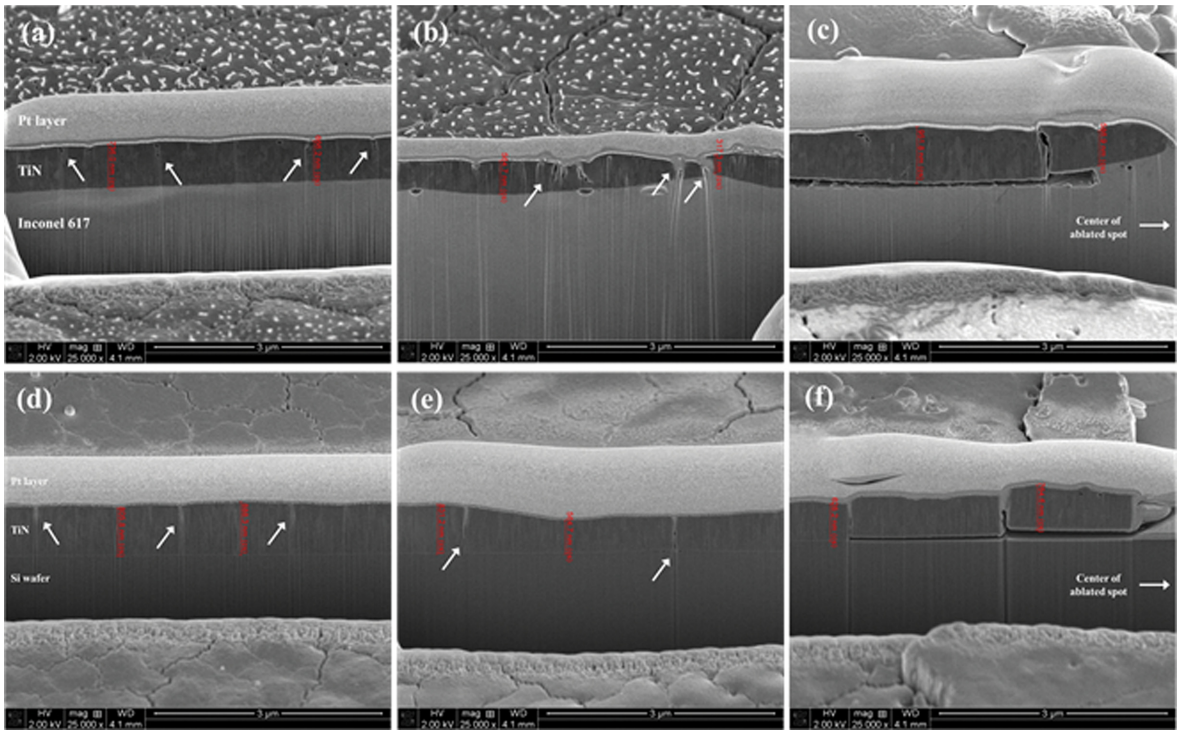

Fig. 7. Cross-sections of laser-ablated spots on the coating specimens: after (a) 5, (c) 9, (e) 15 pulses to TiN on Inconel 617, (d) 9, (e) 15, (f) 20 pulses to TiN on Si wafer.

As seen in Fig. 7(c) and (d), it was revealed that the delamination of the coating layers occurred from the center to the outside of the ablated spots in the TiN/Si specimen, similar to Fig. 6(d) - the TiN/Inconel 617 specimen, by the shear stress from the center of spots. In the TiN/Si specimen, the coating layer showed higher thermal shock resistance due to its low thermal conductivity and the interfacial cracks was formed as our previous study revealed [20]; when compressive stress was applied to the coating layer due to the lower CTE value of the Si wafer than the TiN coating, the dominant crack propagation behavior was interfacial cracking [26-29].

4. Conclusions

The finite element analysis and the experimental data of the degradation behaviors of the TiN coating on the different substrate materials were investigated after the pulsed laser thermal shock with the microstructural observation. The FEA results showed that the heat accumulation at the center of the spot and the mechanical stress to the outside of the spot was occurred by the thermo-mechanical stresses. In the experimental data, the surface melting in the TiN/Inconel 617 specimen was identified, and the interfacial cracking was observed in the TiN/Si specimen where the compressive stress was induced. The mechanical stress from the center to the outside of the ablated spots caused the delamination of coating layer in both coating specimens. It was identified that the higher thermal conductivity of the substrate can improve the thermal shock resistance of the coating/substrate system. Further studies about effects of physical properties of substrate materials and a condition of pulsed laser ablation on the degradation behaviors of coating layers will be necessary to predict the coating failure of various coating specimens.

Acknowledgement

This work was supported by a 2-Year Research Grant of Pusan National University.

References

[1] H. Cho and B.W. Lee, “High temperature properties of surface-modified hastelloy X alloy”, J. Korean Cryst. Growth Cryst. Technol. 22 (2012) 183.
[2] W.D. Münz, “Titanium aluminum nitride films: a new alternative to TiN coatings”, J. Vac. Sci. Technol. A 4 (1986) 2717.
[3] O. Knotek, W.D. Münz and T. Leyendecker, “Industrial deposition of binary, ternary, and quaternary nitrides of titanium, zirconium, and aluminum”, J. Vac. Sci. Technol. A 5 (1987) 2173.
[4] A. Krella and A. Czyzniewski, “Influence of the substrate hardness on the cavitation erosion resistance of TiN coating”, Wear 263 (2007) 395.
[5] T. Cselle and A. Barimani, “Today’s applications and future developments of coatings for drills and rotating cutting tools”, Surf. Coat. Technol. 76-77 (1995) 712.
[6] B. Navinšek, “Improvement of cutting tools by TiN PVD hard coating”, Mater. Manuf. Process. 7 (1992) 363.
[7] M.T. Tilbrook, D.J. Paton, Z. Xie and M. Hoffman, “Microstructural effects on indentation failure mechanisms in TiN coatings: Finite element simulations”, Acta Mater. 55 (2007) 2489.
[8] Y. Massiani, A. Medjahed, J.P. Crousier, P. Gravier and I. Rebatel, “Corrosion of sputtered titanium nitride films deposited on iron and stainless steel”, Surf. Coat. Technol. 45 (1991) 115.
[9] S.V. Hainsworth and W.C. Soh, “The effect of the substrate on the mechanical properties of TiN coatings”, Surf. Coat. Technol. 163 (2003) 515.
[10] J.H. Huang, C.Y. Hsu, S.S. Chen and G.P. Yu, “Effect of substrate bias on the structure and properties of ion-plated ZrN on Si and stainless steel substrates”, Mater. Chem. Phys. 77 (2002) 14.
[11] Y. Choi, S. Jeon, M.S. Jeon, H.G. Shon, H.H. Chun, Y.S. Lee and H. Lee, “Crack propagation behavior of TiN coatings by laser thermal shock experiments”, Appl. Surf. Sci. 258 (2012) 8752.
[12] S. Jeon, J. Ha, Y. Choi, I. Jo and H. Lee, “Interfacial stability and diffusion barrier ability of $Ti_{1-x}Zr_xN$ coatings by pulsed laser thermal shock”, Appl. Surf. Sci. 320 (2014) 602.
[13] S. Jeon, B. Kim, Y. Choi, I. Jo and H. Lee, “Thermal shock behaviors of $Ti_{1-x}Zr_xN$ coatings by accelerated test based on pulsed laser ablation”, Ceram. Int. 42 (2016) 2241.
[14] S.L. Soo, D.K. Aspinwall and R.C. Dewes, “3D FE modelling of the cutting of Inconel 718”, J. Mater. Process. Technol. 150 (2004) 116.
[15] E. Ceretti, M. Lucchi and T. Altan, “FEM simulation of orthogonal cutting: serrated chip formation”, J. Mater. Process. Technol. 95 (1999) 17.
[16] K.D. Bouzakis, F. Klocke, G. Skordaris, E. Bouzakis, S. Gerardis, G. Katirtzoglou and S. Makrimallakis, “Influence of dry micro-blasting grain quality on wear behavior of TiAlN coated tools”, Wear 271 (2011) 783.
[17] P. Peyre, I. Chaieb and C. Braham, “FEM calculation of residual stresses induced by laser shock processing in stainless steels”, Model. Simul. Mater. Sci. Eng. 15 (2007) 205.
[18] J.H. Lee, C.D. Yoo and Y.S. Kim, “A laser-induced thermal spray printing process for phosphor layer deposition of PDP”, J. Micromech. Microeng. 17 (2007) 258.
[19] S. Jeon, C.J. Van Tyne and H. Lee, “Degradation of TiAlN coatings by the accelerated life test using pulsed

laser ablation", Ceram. Int. 40 (2014) 8677.
[20] S. Jeon, H. Lee, I. Jo, D. Shin and K.S. Lee, "Degradation of TiN coatings on Inconel 617 and silicon wafer substrates under pulsed laser ablation", J. Mater. Eng. Perform. 23 (2014) 1651.
[21] K. Ding and L. Ye, "FEM simulation of two sided laser shock peening of thin sections of Ti-6Al-4V alloy", Surf. Eng. 19 (2003) 127.
[22] N.A. Sakharova, J.V. Fernandes, M.C. Oliveira and J.M. Antunes, "Influence of ductile interlayers on mechanical behavior of hard coatings under depth-sensing indentation: a numerical study on TiAlN", J. Mater. Sci. 45 (2010) 3812.
[23] D. Stone, K. Yoder and W. Sproul, "Hardness and elastic modulus of TiN based on continuous indentation technique and new correlation", J. Vac. Sci. Technol. A 9 (1991) 2543.
[24] N.K. Seo, S. Jeon, Y. Choi, M.S. Jeon, H.G. Shin and H. Lee, "Interfacial characteristics of TiN coatings on SUS304 and silicon wafer substrates with pulsed laser thermal shock", Korean J. Met. Mater. 52 (2014) 81.
[25] Q. Lu, S.S. Mao, X. Mao and R.E. Russo, "Delayed phase explosion during high-power nanosecond laser ablation of silicon", Appl. Phys. Lett. 80 (2002) 3072.
[26] J. Haider, M. Rahman, B. Corcoran and M.S.J. Hashmi, "Simulation of thermal stress in magnetron sputtered thin coating by finite element analysis", J. Mater. Process. Technol. 168 (2005) 36.
[27] H. Oettel and R. Wiedemann, "Residual stresses in PVD hard coatings", Surf. Coat. Technol. 76-77 (1995) 265.
[28] M. Bielawski, "Residual stress control in TiN/Si coatings deposited by unbalanced magnetron sputtering", Surf. Coat. Technol. 200 (2006) 3987.
[29] C. Kirchlechner, K.J. Martinschitz, R. Daniel, M. Klaus, C. Genzel, C. Mitterer and J. Keckes, "Residual stresses and thermal fatigue in CrN hard coatings characterized by high-temperature synchrotron X-ray diffraction", Thin Solid Films 518 (2010) 2090.